Title

EVALUATION OF FLUXES AND DOSE-EQUIVALENT RATES IN NEUTRON FIELDS AROUND HIGH ENERGY PROTON ACCELERATORS

Author

Rindi, Alessandro.

Publication Date

1968-08-01

University of California

Ernest O. Lawrence Radiation Laboratory

EVALUATION OF FLUXES AND DOSE-EQUIVALENT RATES IN NEUTRON FIELDS AROUND HIGH ENERGY PROTON ACCELERATORS

Alessandro Rindi

August 1968

Berkeley, California

For Health Physics Society
Midyear Topical Symposium,
Los Angeles, Jan. 29-31, 1969

UCRL-18424

UNIVERSITY OF CALIFORNIA

Lawrence Radiation Laboratory
Berkeley, California

AEC Contract No. W-7405-eng-48

EVALUATION OF FLUXES AND DOSE-EQUIVALENT RATES IN NEUTRON FIELDS AROUND HIGH ENERGY PROTON ACCELERATORS

Alessandro Rindi

August 1968

EVALUATION OF FLUXES AND DOSE-EQUIVALENT RATES IN NEUTRON FIELDS AROUND HIGH ENERGY PROTON ACCELERATORS

Alessandro Rindi

Lawrence Radiation Laboratory
University of California
Berkeley, California

August 1968

ABSTRACT

An analysis is made of the errors involved in routine measurements of flux and dose equivalent around high-energy accelerators. By use of some typical neutron spectra from multidetector measurements made around the accelerators at the Lawrence Radiation Laboratory, Berkeley, and the proton synchrotron at CERN, Geneva, a calculation is made of the errors involved when only one detector is used for evaluating the total neutron flux and corresponding dose-equivalent rate. The correction factors to be applied to the routine measurements in these fields have been calculated, and a method is proposed for minimizing those errors. A CDC-6600 computer was used to make the calculations.

INTRODUCTION

A routine measurement made only for purposes of radiation protection has to be as simple and as quick as possible, has to employ a minimum quantity of instrumentation, and has to permit an evaluation of the dose equivalent with no greater error than allowed by the ICRP. However, such measurements should also give some information about the physical parameters of the radiation so that protective measures can be taken. Not much choice exists in the instrumentation which can be utilized and which copes with routine needs: all users are confined to more or less sophisticated moderated BF_3 counters, a few activation detectors (generally C, S, In or Au, Al, etc.), and TE ionization chambers.

However, slightly different methods are used at different accelerator centers for evaluating from the routine measurements the total dose equivalent in the mixed neutron fields. The differences between the various centers are mainly in the interpretation of the data and in the philosophy of the measurement. Certain laboratories are mainly concerned with the final extrapolation of the instrument readings into the dose equivalent or the "risk involved," the intermediate step of the analysis of the quality of radiation being used only to confirm that the dose-equivalent evaluation has been made with acceptable precision. However, the probable errors seem to be quite high.[3]

At the Lawrence Radiation Laboratory a knowledge of the distribution of the different radiations in the field[1]--i.e., the description of the field in physical terms--is as important as the final evaluation of the dose equivalent. However, this knowledge cannot be gained without using several radiation detectors intelligently selected, and such involved techniques cannot be used in all routine measurements.

Several complete radiation measurements[2] performed around different proton accelerators have supplied us with a group of neutron spectra which we believe to be representative of those around most accelerators. Using these spectra, we calculate for each of the detectors normally employed around accelerators the percent of flux and dose that falls within its sensitivity range, and the percentage errors one normally makes in evaluating flux and dose in these fields. Next, by minimizing these errors, we calculate the best average cross-section and flux-to-dose conversion factor to be used for routine measurements.

From the ratios of the readings of two or three of these detectors, one can select the most probable spectrum (among those considered) that agrees with the measured ratios and then use the cross sections and conversion factors appropriate for this spectrum.

It is worth emphasizing that the sine qua non of this or any other method of analyzing errors in dose-equivalent estimates is a description of the radiation field in physical terms.

The Spectra

In Figs. 1 through 5 we show the five main differential neutron spectra we used for the calculations. Four of these are taken from Ref. 2, and we have added a 1/E distribution. We believe these to fairly represent the spectra normally found around particle accelerators.

The following assumptions were adopted in the calculations:

a. Measurements of the selected spectra did not extend to the thermal region. For this reason we extended the spectrum from the minimum energy measured to thermal energies with a straight line. Doing this is supported by the theory of diffusion and thermalization of neutrons in homogeneous media; also some measurements made around CERN accelerators[10] roughly confirm it, as do unpublished measurements at LRL.

b. To simulate the possible situation around other accelerators of different energies, we terminate the spectra at various maximum energies, i.e., 27 MeV, 1.1 GeV, 11 GeV, and the maximum set by the energy of each accelerator where the measurements were made (except for the cosmic ray spectrum). We have constructed 16 different spectra. (In the tables, we refer to them by progressive numbers. See Table II.)

The Detectors

We have selected a few of the detectors most used for the dosimetry around accelerators.[4,5] They are:

a. The bare BF_3 gas-filled proportional counter.

b. The BF_3 counter moderated by 6 cm of paraffin and Cd-covered.

c. The following activation detectors: S, C, Al, Bi, Hg.

Unfortunately, tissue-equivalent ion chambers and detectors which measure quality factors are not susceptible of this analysis and are not included. In Figs. 6 through 9 we show the cross sections we used for the calculation with the listed detectors. We describe in the figure captions the assumptions used for plotting these cross sections.

The Calculations

We used the CDC-6600 computer at the Lawrence Radiation Laboratory for performing the calculations. The main computer program (program SANDRO) calculates first, for each detector j and each spectrum i, the following expressions:

$$A_{i,j} = \frac{\int_{E_j}^{E'_j} \Phi_i\ (E)\ dE}{\int_{E_i(min)}^{E_i(max)} \Phi_i\ (E)\ dE} \times 100, \qquad (1)$$

where E_j and E'_j are the energy limits of sensitivity of the detector j, and $E_i(min)$ and $E_i(max)$ are the lower and upper energy limits of the spectrum i. This value indicates the percent of the total integral flux which falls in the sensitivity range of the detector;

$$B_{i,j} = \frac{\frac{1}{\sigma_j} \cdot \int_{E_j}^{E'_j} \Phi_i(E) \cdot \sigma_j(E) dE}{\int_{E_i(min)}^{E_i(max)} \Phi_i(E)\ dE} \times 100, \qquad (2)$$

where $\sigma_j(E)$ is the cross-section function for the detector j and σ_j is the value of this function that is normally used for the routine measurements[4,11] (see Table I). This expression would give the percent of the flux in the spectrum which is estimated from this detector; this expression does not have a very useful practical meaning, but it is used for further calculations;

$$C_{i,j} = \frac{\int_{E_j}^{E'_j} \Phi_i(E)\cdot D(E)\cdot dE}{\int_{E_i(\min)}^{E_i(\max)} \Phi_i(E)\cdot D(E)\cdot dE} \times 100, \qquad (3)$$

where D(E) is the assumed dose-to-flux relationship as function of neutron energy. (This is the relationship first formulated by R. Thomas (SLAC) and adopted at LRL.[1,2] It seems to be a realistic one in the present state of knowledge, and further offers the advantage that it can be represented analytically.) This expression indicates the percent of the total dose which falls in the sensitivity range of the detector;

$$D_{i,j} = \frac{D\cdot\frac{1}{\sigma_j}\cdot\int_{E_j}^{E'_j} \Phi_i(E)\sigma_j(E)dE}{\int_{E_i(\min)}^{E_i(\max)} \Phi_i(E)\cdot D(E)dE} \times 100, \qquad (4)$$

where D is the value of the flux-to-dose relationship which has been selected for transforming into dose the flux measured with the detector j (see Table I). The same comments as for expression (2) apply here.

Measurement of the Fluxes

In Table II are shown the values of expression (1) calculated for all the different spectra and detectors. The percentage error for each instrument and each spectrum is then calculated. This is given by

$$PE_{i,j} = \frac{\frac{1}{\sigma_j}\int_{E_j}^{E'_j} \Phi_i(E)\sigma_j(E)dE - \int_{E_j}^{E'_j} \Phi_i(E)dE}{\int_{E_j}^{E'_j} \Phi_i(E)dE} \times 100, \qquad (5)$$

and the values are shown in Table III. By minimizing these errors a new value of σ_j is found which, for all the spectra, leads to the best cross section to be used for approximating the true flux. These values are given in Table IV. The new percentage errors are then calculated and shown in Table V. These are the best approximation one can obtain in the flux evaluation with the different detectors for the spectra used.

Measurement of the Doses

In Table VI are shown the values of expression (3) calculated for the different spectra and detectors. The evaluation of the dose equivalent in the region of sensitivity of each detector is normally executed by multiplying the flux by an appropriate flux-to-dose conversion factor. The factors used till now for this evaluation for the different detectors are shown in Table I. The percentage errors made for different spectra and for each detector by using the old cross sections and conversion factors of Table I are shown in Table VII.

By using the corrected cross sections, these errors are minimized and new appropriate conversion factors are found.

In Table IV we show the corrected factors and in Table VIII the final percentage errors. The values on Table VIII represent the best approximation to the dose that can be obtained with the different detectors for the spectra used.

Consequences

From Table II one can see that, as far as flux measurement is concerned, the BF_3 moderated counter is the most effective. Its range of sensitivity varies between 54% and 99% of the integral spectra used. The percentage error in the flux evaluation, which ranged between -10 and -43%, can be reduced by using the more appropriate cross sections proposed to -28 to +16%, which is an acceptable range. However, with respect to the dose evaluation, one can see from Table VI that for certain hard spectra the percent of dose measured can be as low as 17%; the percentage errors were spread between -56% and +117% and can be optimized only to between -70% and +54%. This would mean the necessity of introduction of a safety factor greater than 2, if only a BF_3 moderated counter were used for a dose evaluation in an unknown field. A better dose evaluation, as far as percentage error and percent of total dose detected are concerned, is furnished by the ^{12}C method (minimum percent of dose detected 27%, and optimized percentage errors between -43% and +10%) or the Bi fission detector (minimum percent of dose detected 26%, and optimized percentage errors between -18% and +19%). Such detectors, however, would not be suitably sensitive in low-energy fields and would further require an improvement in sensitivity before giving statistically reliable measurements in very-low-intensity fluxes.

It is evident that none of these detectors can be used alone to give an acceptable dose evaluation in an unknown neutron field. When measuring around high energy accelerators, the dose sensitivity range as well as the percentage errors in dose evaluation for the BF_3 counter are too much in error and, to supplement it, high energy detectors like ^{12}C or Bi fission become advisable.

Conclusions

Simultaneous use of more than one detector seems to be essential when acceptable evaluations of dose rate must be made in high energy neutron fields.

By inspecting the ratio of the readings of two or more detectors one can select a spectrum which best approximates that in which the measurements were made. Once a spectrum has been selected, use of the values in Tables VIII and VI allows the correct value of the dose rate to be calculated from the instrument readings.

To illustrate this we have chosen three methods of detection: a BF_3 bare counter, a moderated BF_3 counter, and ^{12}C activation. For these detectors we calculated the ratios of the measured fluxes (with the new cross sections) and measured doses (with the old cross sections and flux-to-dose conversion) for the different spectra. They are shown in Table IX. The values of these ratios give evidence of being different enough to allow a selection of the most probable spectrum, even though the experimental errors in the measurements are substantial. In Table X we also show the ratios of the measured fluxes (when available) or measured dose rates as evaluated with the three instruments, from certain surveys in which these three instruments were simultaneously employed. Unfortunately, only a few reliable measurements made with the three detectors simultaneously have been reported, and measurements of the thermal neutrons, especially, are very uncertain.

This work is far from being complete. Many more (and more complete) typical spectra have to be introduced into the calculations, and many more reliable survey results have to be used for comparing with theory. Then the correction values in the dose and the flux evaluations will be improved. We consider, however, that the ones proposed here already ameliorate the lack of precision in routine radiation protection measurements around high energy accelerators.

Acknowledgments

I thank H. Wade Patterson, Head of the LRL Health Physics Department, for encouraging this work and offering valued suggestions, and Jorma Routti for the discussions and the essential help in making the programs for the CDC-6600 computer.

This work was done under auspices of the U. S. Atomic Energy Commission.

References

1. H. Wade Patterson, Accuracy of Very-High-Energy Radiation Monitoring, in Proceedings of the European Nuclear Energy Agency Symposium on Radiation Dose Measurements, Their Purpose, Interpretation and Required Accuracy in Radiological Protection, Stockholm, 1967.
2. W. S. Gilbert, H. W. Patterson, and A. R. Smith, Accelerator Neutron Spectra and Spectra to Dose Conversion, UCRL-18076, Feb. 1968.
3. A. Rindi and F. Hoyer, A Rough Estimation of Some Systematic Errors Involved in the Measurement of the DE by the Method of Many Detectors, CERN Internal Report HP/67/30, March 1967.
4. J. B. McCaslin, H. W. Patterson, A. R. Smith, and L. D. Stephens, Some Recent Developments in Technique for Monitoring High-Energy Accelerator Radiations, in Proceedings of the First International Congress of the International Radiation Protection Association, Rome, 1966.
5. M. Yamashita, L. D. Stephens, A. R. Smith, and H. W. Patterson, Detection Efficiency of Bare and Moderated BF_3-Gas-Filled Proportional Counters for Isotropic Neutron Fluxes, J. Nucl. Sci. Technol. 3, No. 8, pp. 343-353 (1966).
6. D. J. Hughes and R. B. Schwartz, Neutron Cross Sections, BNL-325 (1958).
7. W. S. Gilbert et al., 1966 CERN-LRL-RHEL Shielding Experiment at the CERN Proton Synchrotron, UCRL-17941, Nov. 1967.

8. K. Goebel, A. Rindi, A. H. Sullivan, and J. Baarli, The Purpose, Interpretation, and Utilization of Area Monitoring Measurements Near the CERN Accelerators, in Proceedings of the ENEA Symposium on Radiation Dose Measurements, Their Purpose, Interpretation and Required Accuracy in Radiological Protection, Stockholm, 1967.

9. K. Goebel, private communication from CERN-PS survey report of May 1968.

10. D. Nachtigall, The Contribution of Intermediate Energy Neutrons to the DE Outside the Shielding of High Energy Accelerators, CERN Internal Report, ISR/Int-BT/66-16.

11. S. Charalambus, J. Dutrannois, and K. Goebel, Particle Flux Measurements with Activation Detectors, CERN Internal Report DI/HP/90, July 1966.

Table I. Average cross sections (σ_j) and average flux-to-dose conversion factors (D) used in the text for calculating the expressions $B_{i,j}$ (percent flux measured) and $D_{i,j}$ (percent dose measured).

Detector	Average cross section (mb)	Average flux-to-dose ratio (ncm^{-2} sec^{-1}/mrem/h)
BF_3 bare counter	4×10^6 [a]	232
BF_3 moderated counter	1 (relative value)	8
^{115}In (bare)	2×10^5	232
^{32}S	20	10
^{12}C	22	12.8
$^{27}Al\rightarrow^{24}Na$	15	5
$^{27}Al\rightarrow^{22}Na$	10	5
Bi fission	150	5
Hg→Tb	1	1.6

a. Cross section of ^{10}B, weighted for the % in the counter, at 0.025 eV.

Table II. Percent of true flux (expression $A_{i,j}$ in text).

Spectrum	Energy at which terminated	Spectrum No.	Detector: Bare BF_3	In	BF_3 Moder.	S	Al→ ^{24}Na	^{12}C	Al→ ^{22}Na	Bi	Hg
1/E	100 GeV	1	67	67	54	37	32	29	28	28	18
	11 GeV	2	72	72	58	33	27	23	22	22	12
	1.1 GeV	3	78	78	63	27	21	16	15	15	4
	27 MeV	4	92	92	68	14.6	7.8				
CERN ring top	30 Gev	5	18	18	64	92	81	66	61	61	14
	11 GeV	6	18	18	64	92	81	66	61	61	14
	1.1 GeV	7	19	19	68	92	80	64	58	58	8.4
	27 MeV	8	41	41	99	83	58				
Bevatron	27 GeV	9	71	71	80	41	29	19	17	17	3.4
	1.1 GeV	10	71	71	81	41	28	18	16	16	2.3
	27 MeV	11	83	83	87	31	16				
Cosmic ray		12	89	89	87	23	10	6.8	6.2	6.2	1.6
CERN PS Bridge	30 GeV	13	65	65	69	44	34	25	23	23	5
	11 GeV	14	65	65	70	44	34	25	23	23	5
	1.1 GeV	15	66	66	71	43	33	23	21	21	3
	27 MeV	16	82	82	77	29	17				

Table III. Percentage errors in flux (with old cross sections) (expression $PE_{i,j}$ in text).

Spectrum	Bare BF_3	In	BF_3 Moder.	S	$Al \rightarrow {}^{24}Na$	${}^{12}C$	$Al \rightarrow {}^{22}Na$	Bi	Hg
	Detector								
1	-83	+166	-21	+195	+ 20	- 5.3	+34	-21	- 1.3
2	-83	+166	-21	+248	+ 35	- 6.6	+45	-27	- 1.9
3	-83	+166	-20	+348	+ 67	- 9.7	+70	-42	-58
4	-83	+166	-15	+798	+277				
5	-99	- 80	-43	+322	+ 69	-10	+82	-50	-17
6	-99	- 80	-43	+323	+ 69	-10	+83	-50	-17
7	-99	- 80	-43	+349	+ 78	-11	+91	-56	-65
8	-99	- 80	-20	+882	+280				
9	-92	+ 22	-18	+502	+119	-14	+83	-55	-24
10	-92	+ 22	-18	+518	+125	-15	+89	-58	-64
11	-92	+ 22	-12	+819	+283				
12	-95	- 26	- 9.2	+446	+106	-13	+76	-50	-14
13	-87	+211	-24	+450	+ 97	-12	+83	-53	-20
14	-87	+211	-24	+451	+ 97	-13	+84	-53	-20
15	-87	+211	-24	+475	+105	-14	+92	-58	-65
16	-87	+211	-15	+879	+276				

Table IV. New average cross sections for flux evaluation and new average flux-to-dose conversion factors.

Detector	Cross section	Flux-to-dose conversion factor
BF_3 bare counter	5.2×10^5	39
^{115}In (bare)	5.1×10^5	17.7
BF_3 moderated counter	0.78 (relative value)	14.5
^{32}S	136	6.5
^{12}C	19.5	3.4
$^{27}Al \rightarrow ^{24}Na$	40	6.4
$^{27}Al \rightarrow ^{22}Na$	17.8	3.5
Bi fission	81.5	3
Hg→Tb	0.78	1.8

Table V. Percentage errors in flux (with new cross sections).

	Detector								
Spectrum	Bare BF_3	In	BF_3 Moder.	S	$Al\to{}^{24}Na$	^{12}C	$Al\to{}^{22}Na$	Bi	Hg
1	+25	+ 4.4	+ 2.1	-56	-54	+6.7	-25	+44	+26
2	+27	+ 4.3	+ 1.7	-49	-49	+5.3	-18	+33	+21
3	+27	+ 4.7	+ 1.7	-34	-38	+1.8	- 3.7	+ 6.4	-47
4	+24	+ 4.1	+ 9.3	+31	+38				
5	-94	-92	-28	-38	-36	+1	+ 2.3	- 8.7	+ 5.7
6	-94	-92	-26	-38	-34	+1	+ 2.6	- 9	+ 5.4
7	-94	-92	-26	-33	-35	0	+ 7.6	-18	-55
8	-94	-92	+ 1	+44	+42				
9	-44	-52	+ 4.1	-10	-19	-4	+ 3	-17	- 2.7
10	-43	-52	+ 4.4	- 9	-16	-4.8	+ 6	-24	-55
11	-43	-52	+12	+34	+42				
12	-65	-62	+16	-18	-21	-2.2	- 1	- 9	+ 9.7
13	- 3.4	+22	- 3.4	-19	-25	-1.6	+ 3	-14	+ 2
14	- 3.4	+22	- 3	-19	-25	-1.6	+ 3	-14	+ 2
15	- 3.7	+22	- 2.5	-16	-23	-2.8	+ 8	-23	-55
16	- 6.6	+22	- 8	+46	+47				

Table VI. Percentage of true dose.

	Detector								
Spectrum	Bare BF_3	In	BF_3 Moder.	S	$Al \rightarrow ^{24}Na$	^{12}C	$Al \rightarrow ^{22}Na$	Bi	Hg
1	8.9	8.9	17	94	91	88	87	87	74
2	15	14	29	91	85	80	79	79	57
3	26	26	51	85	74	65	62	62	23
4	65	65	96	62	34				
5	8.1	8.1	44	98	91	82	78	78	29
6	8.2	8.2	44	98	92	82	78	78	28
7	9.6	9.6	52	97	90	78	74	74	16
8	32	32	99	92	67				
9	34	34	68	83	65	52	48	48	15
10	36	36	72	82	63	49	45	45	9.9
11	62	62	99	69	37				
12	65	65	80	59	35	27	26	26	11
13	21	21	57	90	78	65	62	62	22
14	22	22	57	90	78	65	62	62	22
15	24	24	65	89	75	61	57	57	12
16	52	52	98	76	47				

Table VII. Percentage errors in dose (with old cross sections and conversion factors).

Spectrum	Detector: Bare BF_3	In	BF_3 Moder.	S	$Al \rightarrow {}^{24}Na$	${}^{12}C$	$Al \rightarrow {}^{22}Na$	Bi	Hg
1	-97	-53	+ 65	- 36	- 53	-86	-54	-73	-21
2	-97	-53	+ 65	+ 5	- 26	-82	-31	-65	+ 9.1
3	-97	-53	+ 65	+ 93	+ 30	-75	+15	-60	-39
4	-97	-53	+117	+512	+390				
5	-99	-99	- 56	+ 70	+ 28	-75	+21	-67	+ 1.5
6	-99	-99	- 56	+ 71	+ 30	-75	+22	-67	+ 2.6
7	-99	-99	- 56	+101	+ 51	-72	+43	-70	-48
8	-99	-99	- 27	+553	+390				
9	-99	-89	+ 19	+200	+ 92	-74	+31	-68	+ 1.5
10	-99	-89	+ 19	+223	+110	-73	+44	-68	-47
11	-99	-89	+ 47	+529	+402				
12	-99	-92	+ 65	+192	+ 68	-76	+13	-68	- 1
13	-98	-62	+ 6	+147	+ 61	-75	+25	-68	- 0.8
14	-98	-63	+ 6	+150	+ 62	-75	+26	-68	0
15	-98	-63	+ 6	+183	+ 85	-73	+46	-68	-48
16	-98	-63	+ 45	+563	+391				

Table VIII. Percentage errors in dose (with new cross sections and new conversion factors).

	Detector								
Spectrum	Bare BF_3	In	BF_3 Moder.	S	$Al \rightarrow {}^{24}Na$	^{12}C	$Al \rightarrow {}^{22}Na$	Bi	Hg
1	+33	+20	+20	-85	-86	-43	-63	-18	-13
2	+31	+26	+14	-76	-78	-26	-45	+ 5.6	+20
3	+32	+18	+16	-56	-62	-10	- 6	+19	-33
4	+34	+18	+54	+38	+46				
5	-98	-98	-70	-62	-62	+ 2	- 2	+ 3	+14
6	-98	-98	-70	-61	-62	+ 2	- 1	+ 3	+14
7	-98	-98	-69	-54	-56	+13	+16	+ 0.2	-42
8	-98	-98	-48	+48	+44				
9	-70	-72	-16	-32	-43	+ 5	+ 6	- 3	+15
10	-69	-72	-15	-27	-38	+11	+16	- 4	-43
11	-69	-72	+ 4	+42	+48				
12	-83	-80	+17	-34	-51	- 0.6	-10	- 1.3	+ 9
13	-30	- 2	-25	-44	-52	+ 3	0	- 5	+10
14	-37	- 6	-24	-43	-52	+ 3	+ 1	- 5	+10
15	-43	- 4	-26	-36	-45	+10	+17	- 2	-45
16	-31	- 6	+ 3	+51	+46				

Table IX. Ratios of the measured fluxes and doses for the detectors:

A = BF_3 bare, B = BF_3 mod, C = ^{12}C activation.

	Ratios					
	Flux			Dose		
Spectrum	A/B	A/C	B/C	A/B	A/C	B/C
1	1.52	2.7	1.77	9×10^{-3}	2.2×10^{-2}	2.4
2	1.55	3.7	2.36	9.2×10^{-3}	3.1×10^{-2}	3.3
3	1.54	5.8	3.75	9×10^{-3}	4.7×10^{-2}	5.2
4	1.54			9.1×10^{-3}		
5	2.2×10^{-2}	1.5×10^{-2}	0.7	1.2×10^{-4}	1.1×10^{-4}	0.95
6	2.1×10^{-2}	1.5×10^{-2}	0.71	1.2×10^{-4}	1.2×10^{-4}	0.95
7	2.2×10^{-2}	1.7×10^{-2}	0.78	1.2×10^{-4}	1.4×10^{-4}	1.1
8	2.2×10^{-2}			1.2×10^{-4}		
9	0.48	2.1	4.4	2.7×10^{-3}	1.7×10^{-2}	6.3
10	0.48	2.35	4.9	2.8×10^{-3}	1.8×10^{-2}	6.6
11	0.48			2.8×10^{-3}		
12	0.3	4.5	15	1.7×10^{-3}	3.6×10^{-2}	21
13	0.95	2.5	2.6	5.3×10^{-3}	2×10^{-2}	3.7
14	0.94	2.5	2.7	5×10^{-3}	1.9×10^{-2}	3.8
15	0.91	2.7	3	4.4×10^{-3}	1.9×10^{-2}	4.2
16	0.92			5.5×10^{-3}		

Table X. Some measured ratios.

Location and Reference	A/B	A/C	B/C	Probable spectrum
On the concrete 4-ft roof of the LRL synchrocyclotron. Internal target. p beam 700 MeV (neutron flux measurements with new cross sections).	0.46	2.6	5.6	(10) or (11)
Survey made on the roof of a concrete tunnel surrounding an extracted p beam of 19 GeV/c at CERN PS. (Neutron dose measurements--Ref. 9--with old factors.)	9×10^{-3}	1.2×10^{-2}	1.3	(1)
South experimental hall of CERN PS. At 90° from extracted 19-GeV/c p beam. (Neutron dose measurements--Ref. 8--with old factors.)	6×10^{-2}	2×10^{-1}	3.6	(?) within a factor of 10 for the thermal neutron value, spectrum 13 can fit.
Far from end stop of a p beam of 19 GeV/c at CERN PS. (Neutron dose measurements--Ref. 8--with old factors.)	1.1×10^{-1}	2.1	19	(?) the B/C ratio can fit spectrum 12.

FIGURE CAPTIONS

Fig. 1. Plot of a hypothetical 1/E differential spectrum as used for calculations.

Fig. 2. Differential neutron spectrum measured at the LRL 6.2-GeV Bevatron (Ref. 2). (The spectra in Figs. 2 through 5 have been arbitrarily extended to thermal regions. See text.)

Fig. 3. Differential neutron spectrum measured on the concrete bridge on the ring of the CERN 28-GeV proton synchrotron (Ref. 2).

Fig. 4. Differential neutron spectrum measured on the top of the earth shield at the CERN 28-GeV proton synchrotron (Ref. 2).

Fig. 5. Differential neutron spectrum of cosmic rays measured at LRL (Ref. 2).

Fig. 6. Cross section for the reaction $^{10}B(n,\alpha)^{7}Li$. The values are those given from D. Hughes and R. Schwartz (Ref. 6) for elemental B multiplied by 5.25 for taking into account the ^{10}B enrichment into the counter.

Fig. 7. Simplified shape of the $^{115}In(n,\gamma)^{116}In$ reaction cross section (Ref. 6).

Fig. 8. Efficiency curve of the BF_3 counter, moderated by 6 cm of paraffin and Cd-covered, as measured at LRL (Refs. 5,7). This shape is also approximately valid for the In, Au, and Co moderated detectors.

Fig. 9. Cross sections for the following reactions (Refs. 4,7) as used for the calculations:

a. $^{32}S(n,p)^{32}P$

b. $^{12}C(n,2n)^{11}C$

c. $^{27}Al(n,\alpha)^{24}Na$

d. $^{27}Al(n,spal)^{22}Na$

e. $^{209}B(n,fiss)$ Used in Bi fission chamber

f. $Hg(n,spal)^{149}Tb$

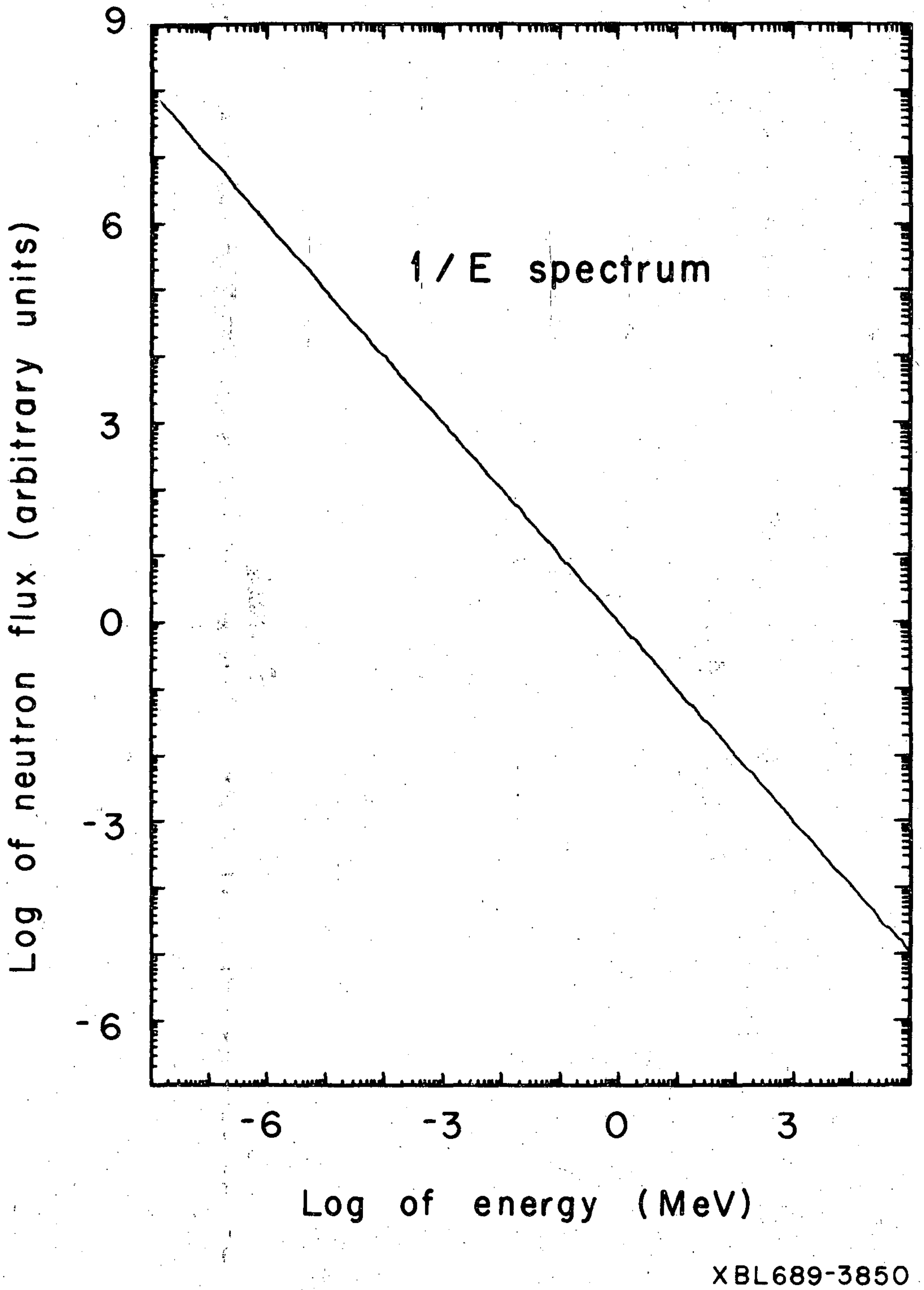
9
6
3
0
-3
-6
Log of neutron flux (arbitrary units)
1/E spectrum
-6
-3
0
3
Log of energy (MeV)
XBL689-3850

Fig. 1

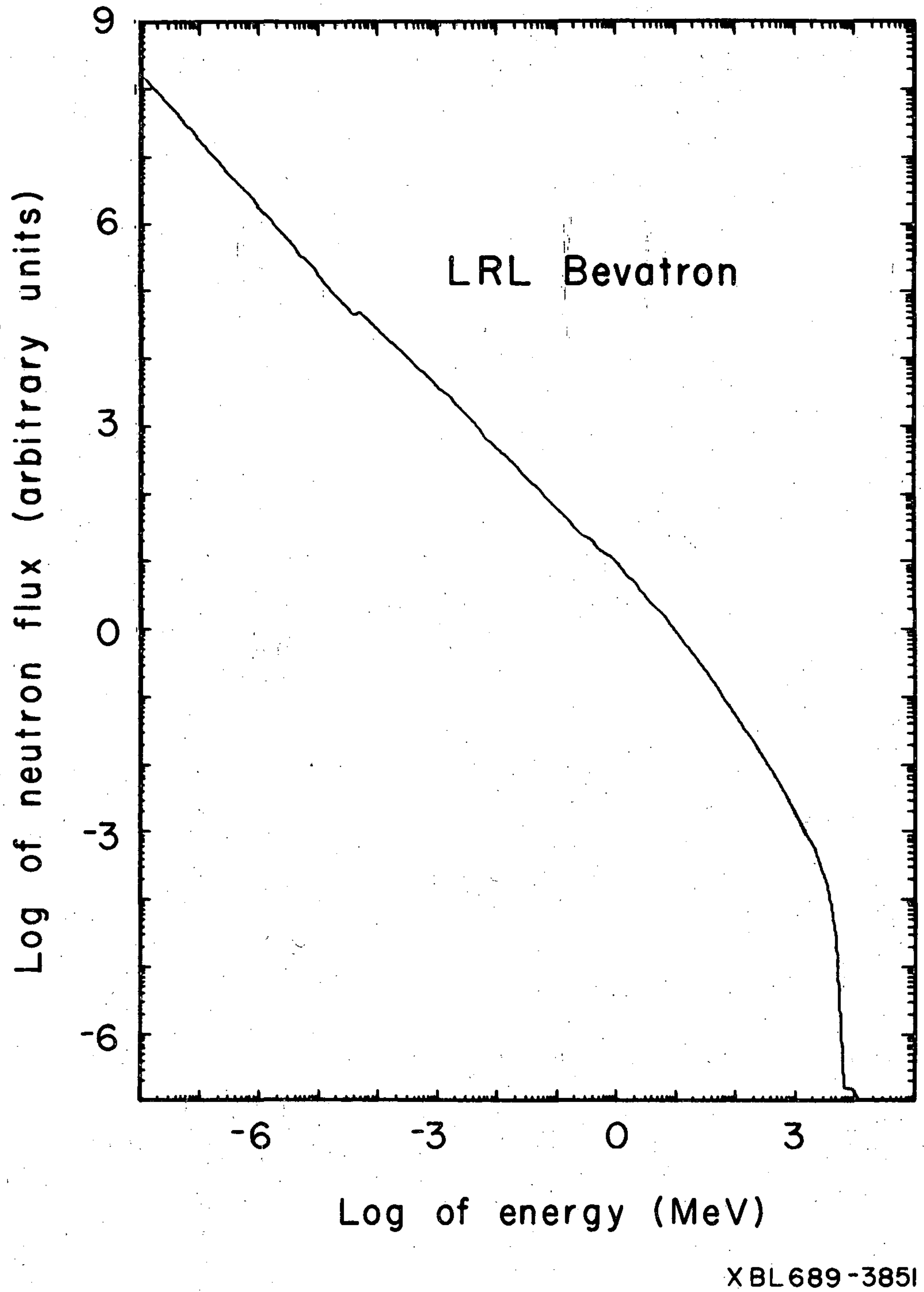
9
6
3
0
-3
-6
Log of neutron flux (arbitrary units)
LRL Bevatron
-6
-3
0
3
Log of energy (MeV)
XBL689-3851

Fig. 2

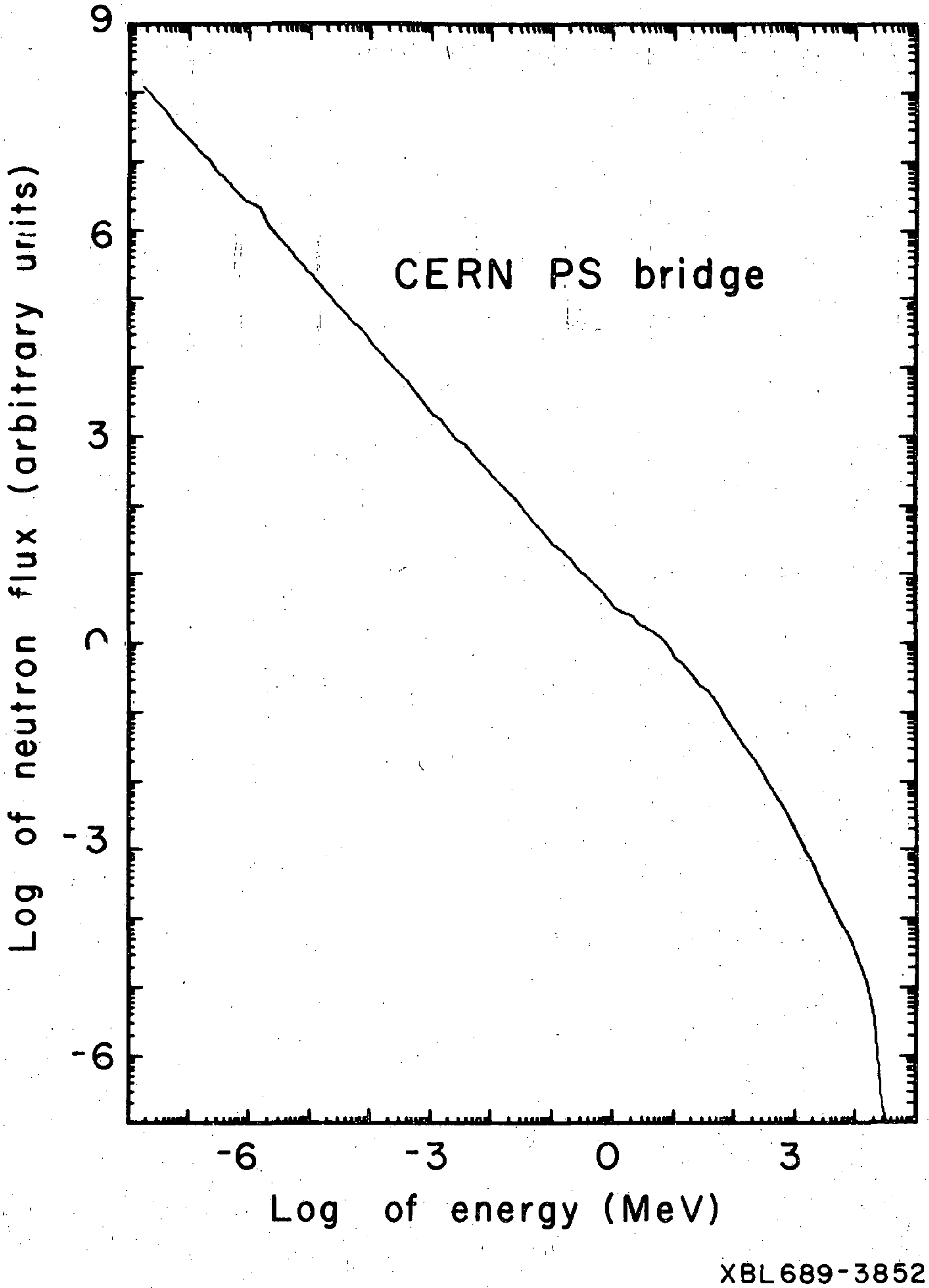
CERN PS bridge
Log of neutron flux (arbitrary units)
Log of energy (MeV)
9
6
3
0
-3
-6
-6
-3
0
3
XBL689-3852

Fig. 3

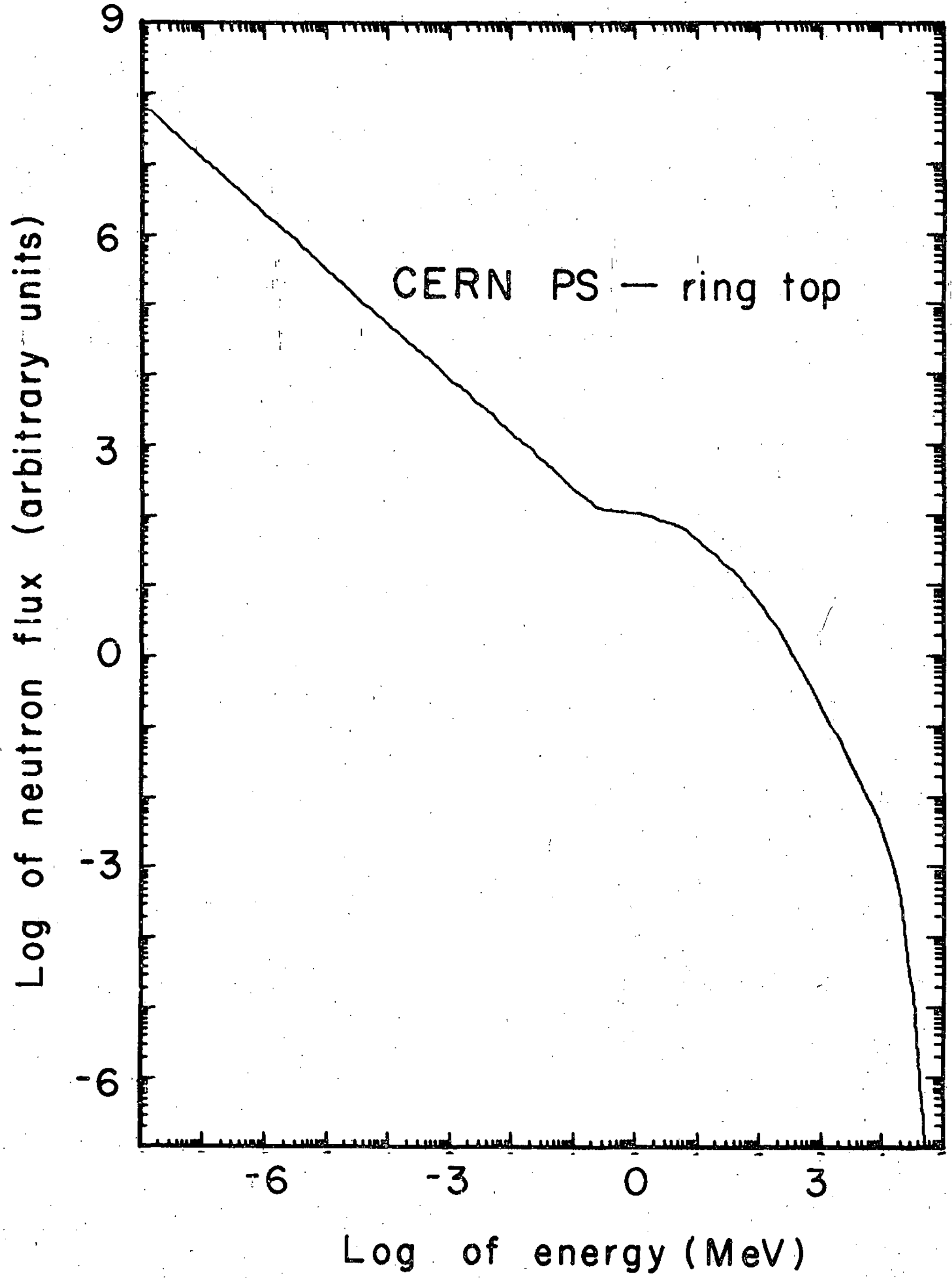

XBL689-3853

Fig. 4

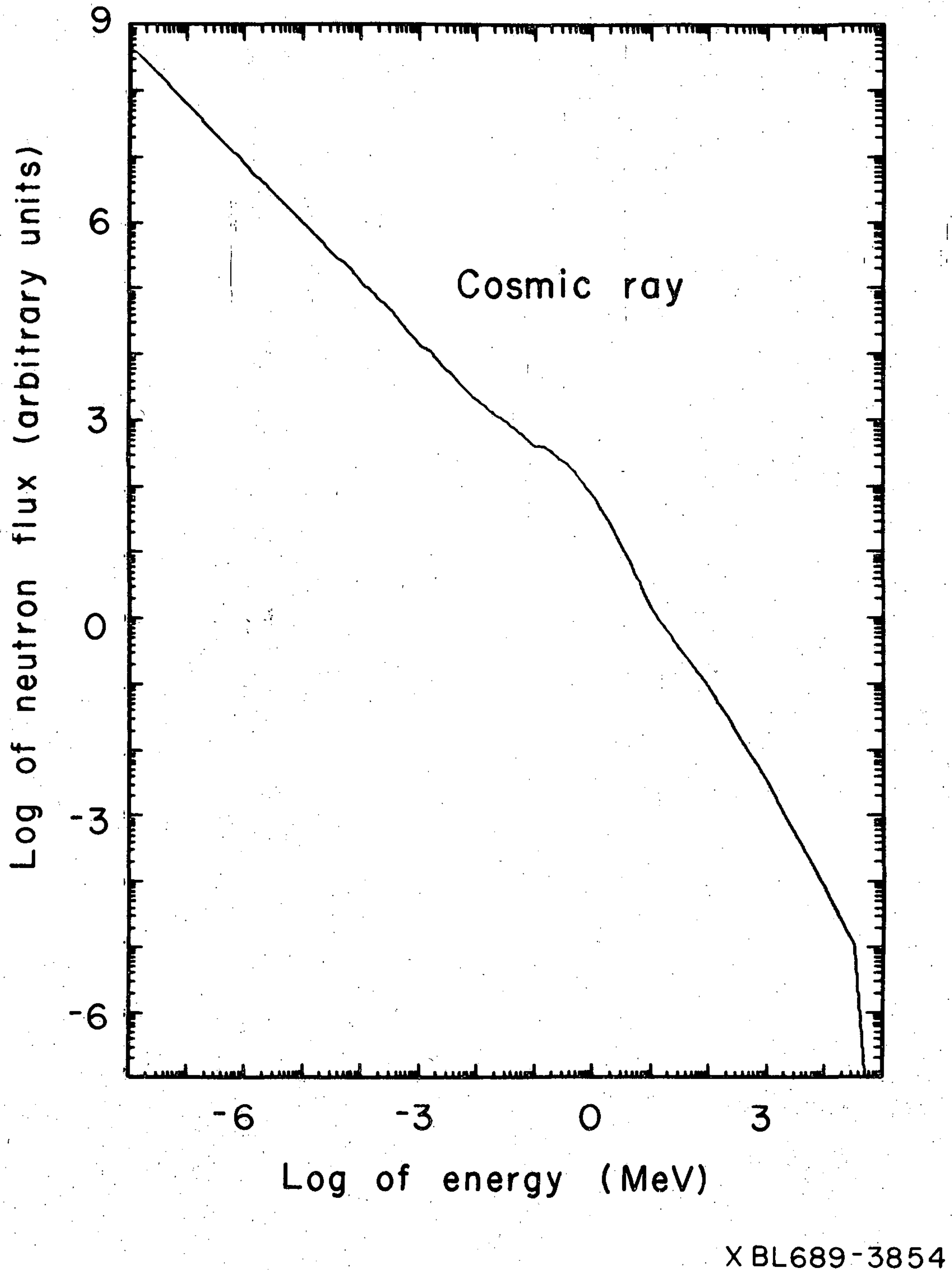
9
6
3
0
-3
-6
Log of neutron flux (arbitrary units)
Cosmic ray
-6
-3
0
3
Log of energy (MeV)
XBL689-3854

Fig. 5

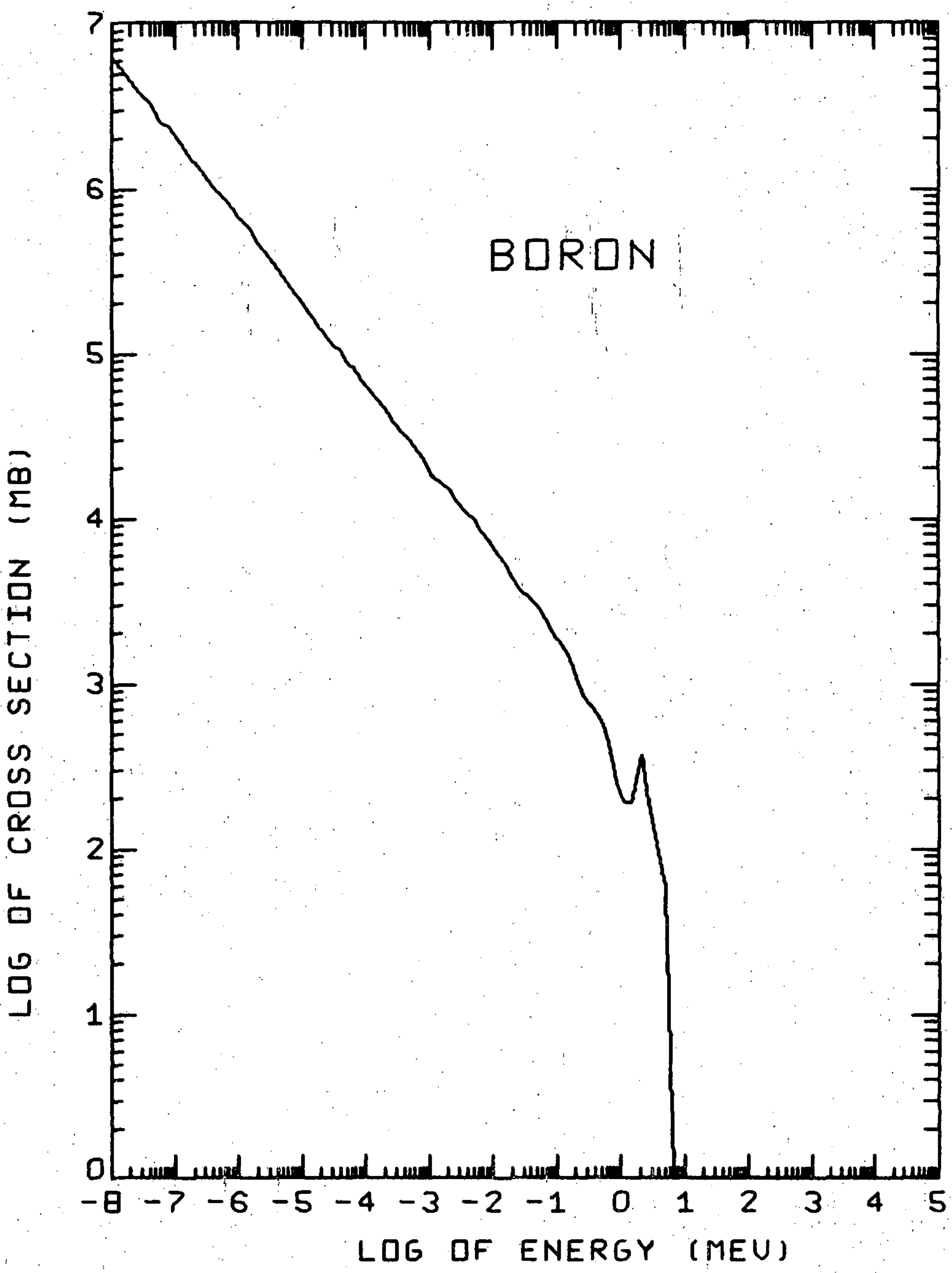

XBL689-3855

Fig. 6

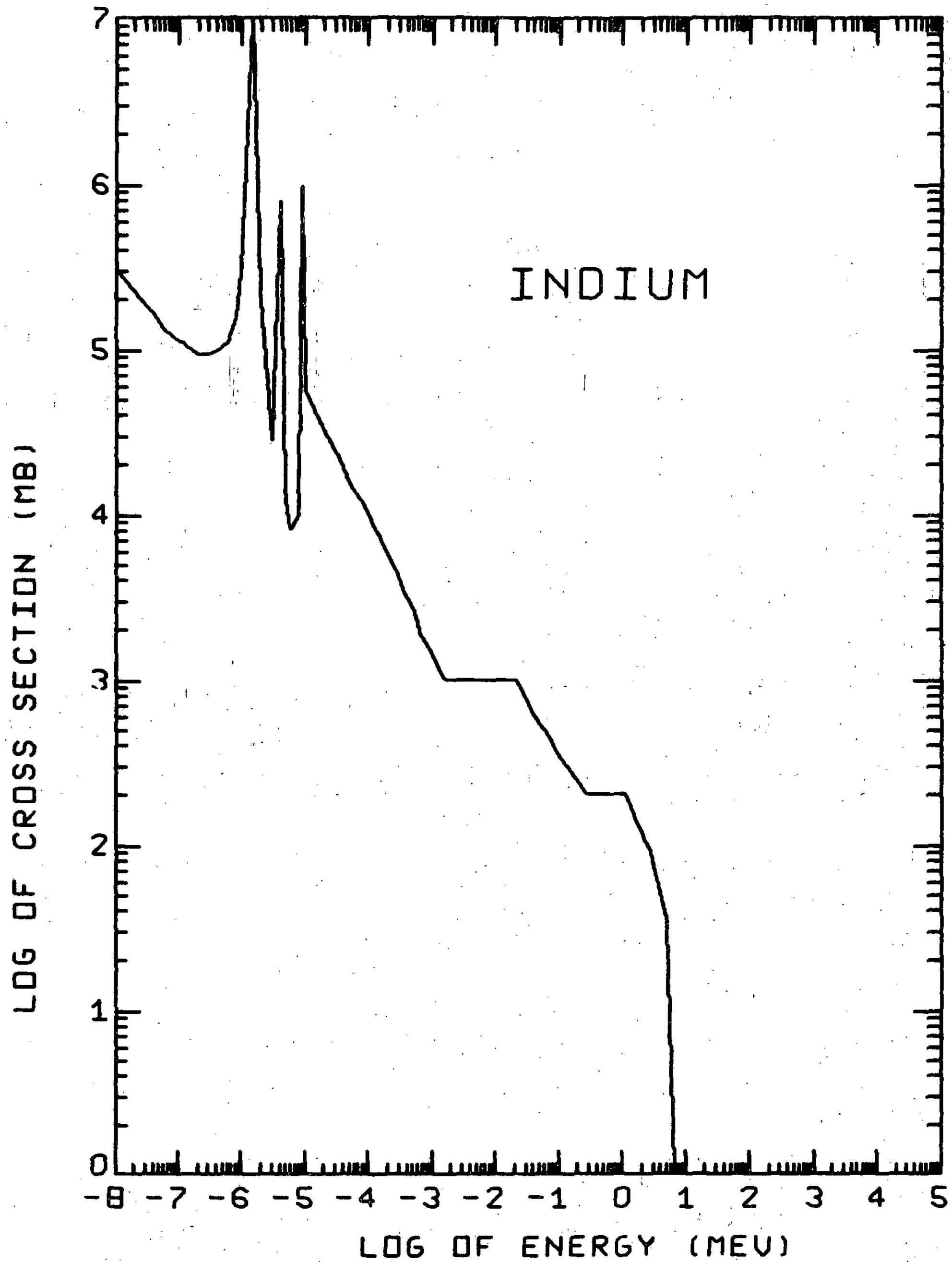

XBL689-3856

Fig. 7

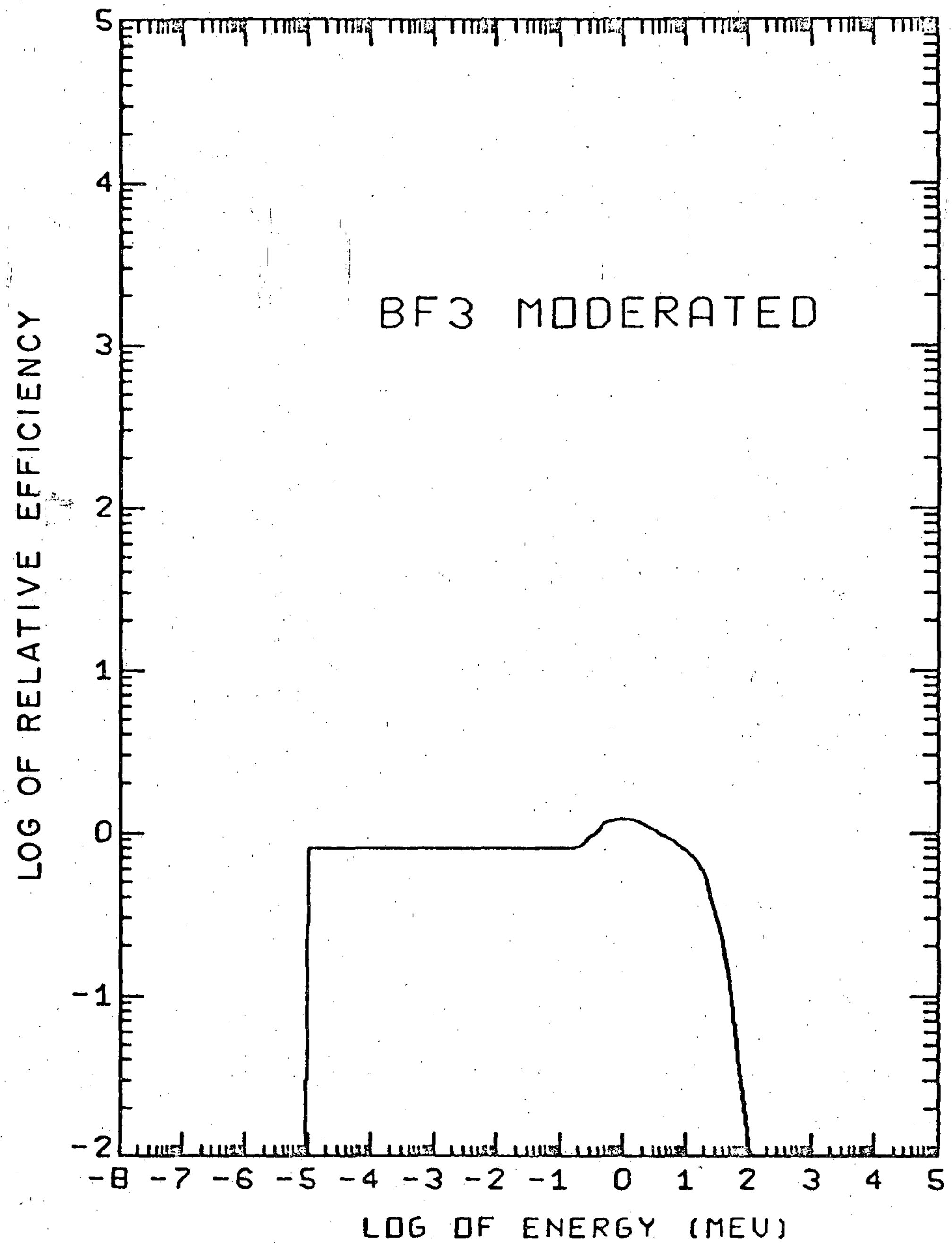
BF3 MODERATED
LOG OF RELATIVE EFFICIENCY
LOG OF ENERGY (MEV)
5
4
3
2
1
0
-1
-2
-8 -7 -6 -5 -4 -3 -2 -1 0 1 2 3 4 5

Fig. 8

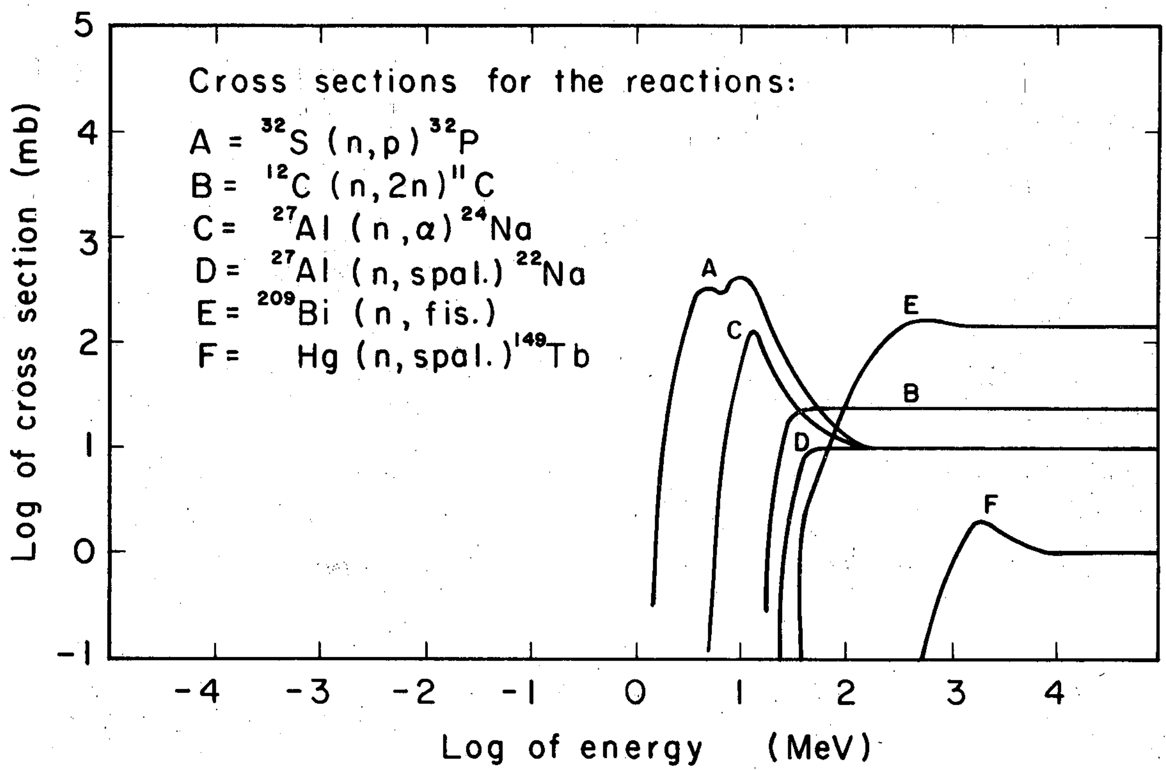

XBL688-3713

Fig. 9